Universiteit Leiden
The Netherlands

Imaging plasma membrane domains in signal transduction pathways

Pezzarossa, A.

Citation

Pezzarossa, A. (2012, March 13). *Imaging plasma membrane domains in signal transduction pathways*. Retrieved from https://hdl.handle.net/1887/18585

Version:	Not Applicable (or Unknown)
License:	Leiden University Non-exclusive license
Downloaded from:	https://hdl.handle.net/1887/18585

Note: To cite this publication please use the final published version (if applicable).

Cover Page

Universiteit Leiden

Leiden University Repository

The handle http://hdl.handle.net/1887/18585 holds various files of this Leiden University dissertation.

Author: Pezzarossa, A.
Title: Imaging plasma membrane domains in signal-transduction pathways
Issue Date: 2012-03-13

Chapter 3

Effects of membrane compartmentalization and subunits relative concentration on type I interferon receptor assembly in living cells[1]

The type I Interferon receptor (Ifnar) is a member of the helical cytokine family. It is a complex heteromeric receptor, which comprises two subunits, Ifnar1 and Ifnar2. Upon stimulation with interferon (IFN) a trimeric complex between the two subunits and the ligand is formed with a 1:1:1 stoichiometry. Although complex assembly has been characterized in great details in model membrane, studies on living cells were lacking. Particularly, knowledge on how an effective recruitment of receptor components in the plane of the membrane is achieved is still lacking. We applied single-molecule fluorescence microscopy to study the lateral organization of extra-cellular domains of both Ifnar1 and Ifnar2 in living HeLa cells. Moreover, we demonstrate the influence of relative concentrations of receptor concentration on subunits mobility, and thus the role of lateral interaction in maintaining the lateral organization of receptor components.

[1]This chapter is based on: Pezzarossa, A., Piehler, J., Schmidt., T. "Effects of membrane compartmentalization and relative concentration on type I interferon receptor assembly in living cells." (in preparation).

3.1 Introduction

The type I interferon family (IFN) comprises 13 different subtypes of IFN-α and one IFN-β. This large variety of IFNs bind to one shared receptor complex (Ifnar), which elicit differential responses, spanning from antiviral responses to cell growth inhibition (1). The type I interferon receptor is a complex heteromeric receptor, composed of two transmembrane proteins, Ifnar1 and Ifnar2. The extra cellular domain (ECD) of Ifnar2 has been characterized by nuclear magnetic resonance and is composed of two fibronectin III (FBNIII)-like domains (2). The ECD of Ifnar1 instead comprises four FBNIII-like subdomains.(3). The intracellular domains (ICDs) of Ifnar1 and IFNaR2 are associated with two cytoplasmic tyrosine kinase, TYK2 and Jak1, respectively (4). Upon ligand binding a signaling ternary complex between Ifnar1, Ifnar2 and IFN is formed, characterized by a 1:1:1 stoichiometry, and the signaling cascade is initiated. In the first stages of signaling, TYK2 and Jak1 reciprocally trans-phosphorylate the receptor chains and STAT1 and STAT2 (Signal Transducers and Activators of Transcription) are recruited from the plane of the membrane and phosphorylate (1).

Differently from other helical cytokines, no pre-assembly of the subunits has been observed, thus suggesting a ligand-induced assembly mechanism (5). Experimentally, this has been confirmed by Gavutis et.al. *in vitro* based on binding studies which monitored the assembly of the ECDs of Ifnar1 and Ifnar2 on solid-supported bilayers (6). The authors proposed a model where the assembly follows a two steps mechanism: first a binary complex between one Ifnar subunits and the ligand is formed and then the second subunit is recruited on the membrane plane. As the affinity of IFNs are generally higher for Ifnar2 than Ifnar1 (with the exception of IFNβ), the probability of formation of a binary complex Ifnar2-IFN is higher than for Ifnar1-IFN. All the interactions between the complex components are transient in nature, thus leading to a dynamic equilibrium between binary and ternary complex. Further studies by Lamken (5) on solid supported membranes, showed how the relative concentration of Ifnar1 and Ifnar2 in the plane of the membrane plays an important role in the formation of stable complexes, suggesting that the complex is stabilized by fast re-association, and its kinetic is concentration dependent (5). From these experiments the rate constants for complex assembly were retrieved. In the work from Gavutis (7), however, it was highlighted how an equilibrium constant of 36 mol/μm^2 is not sufficient for an ef-

fective recruitment of receptor components when these are present at low concentration (∼1000 receptor/cell) uniformly distributed along the membrane of a living cells. Thus, it was suggested that the lateral organization and possibly the confinement into membrane domains could explain the efficient assembly observed *in vivo*.

Here we applied single-molecule fluorescence microscopy to study the lateral organization of the ECDs of Ifnar1 and Ifnar2 in living HeLa cells. We address the question of receptor components confinement, and describe their mobility within the plane of the membrane before and after stimulation with IFN. Moreover, we studied the effect of different relative concentrations of Ifnar1 and Ifnar2 onto their mobility. We found that both Ifnar1 and Ifnar2 are present as two fractions, a fast diffusing one ($\sim 60 - 70\%$) and a slow diffusing ($\sim 30 - 40\%$), confined in domains differing in size of several hundreds nanometers. Further, we show how Ifnar2, but not Ifnar1 confinement is F-actin dependent. Upon stimulation with IFNα2 we observed a significant change in receptor's component mobility. Through cross-correlation experiments, we confirm that only a minor fraction (16%) of receptor appears to be pre-coupled before stimulation.

Finally, we show how different relative concentrations influence the mobility of both Ifnar1 and Ifnar2, suggesting that transient lateral interactions between the different subunits play a fundamental role in the lateral organization of the receptor components.

3.2 Materials and methods

3.2.1 Cell culture and transformation

Human cervix carcinoma epithelial cells (HeLa) were cultured in DMEM medium supplemented with 10% fetal calf serum (FCS), streptomycin (200 μg/ml) and penicillin (200 U/ml) in a 7% CO_2 humidified atmosphere at 37 °C (95% humidity). Cells were transferred every 4 days. For microscopy, cells were cultured on 25 mm ⊘ glass slides, pretreated with hydrogen fluoride. Adherent cells were transfected with 1μg DNA and 3 μl FuGENE 6HD (Roche Diagnostic GmbH, Mannheim, Germany) per glass slide.

3.2.2 Plasmid

The plasmid pVitro2 H10-Ifnar1ΔlC-A1-Ifnar2ΔlC was obtained from the group of Pielher. The stop codon for the gene Ifnar1-ΔlC was removed by cutting the gene with the restriction enzymes BbsI and BamHI and introducing a double-stranded oligomer between these to restriction site (TGCGAAAGTCTTCTTGAGATGCCGCGGATCC). The coding sequence for the fluorescent protein eYFP was obtained by cutting the plasmid pcDNA3 LckN11-eYFP with the restriction enzymes BamHI and XbaI. It was introduced after Ifnar1-ΔlC using the same enzymes to form the plasmid pVitro2 H10-Ifnar1-ΔlC-eYFP-A1-Ifnar2-ΔlC. The promoter for the transcription of the coding sequence of A1-Ifnar2-ΔlC was removed by cutting it out with the restriction enzyme EcoRI. Thus, we obtained the plasmid pVitro2 H10-Ifnar1-ΔlC-eYFP. The DNAs were checked by restriction enzyme digestion and sequencing analysis.

3.2.3 A1-tag labeling

A1-Ifnar2 was expressed transiently in HeLa cells and fluorescently labeled prior to measurements following the protocol given by the manufacturer. As a substrate we choose CoA-647 (New England $\text{BioLabs}_{\text{inc}}$). For single-molecule imaging, the labeling solution was prepared using complete medium (including serum), $MgCl_2$ to a final concentration of 10 mM, 1μM of ACP-Synthase (New England $\text{BioLabs}_{\text{inc}}$) and CoA-647 substrate to a final concentration of $1\mu M$. Cells were incubated for 30 minutes and washed 5 times to remove excess dye. Labeling specificity was tested on non-transfected cells via fluorescent imaging. In non-transfected cells, the signal was lower than 1 molecule/10 μm^2.

3.2.4 IFNα2 stimulation

Cells in a chamber filled with PBS were incubated with 5 nM IFNα2 for 5 minutes. Measurements were performed up to 30 minutes after incubation.

3.2.5 Latrunculin A treatment

Cells in a chamber with PBS were supplemented with 5 μM latrunculin A, and incubated for 10 minutes. Subsequently, they were measured for up to 30 minutes. Prior to each measurement, cells were imaged with bright field to ensure they were viable.

3.2.6 Single-Molecule Microscopy

The setup has been described in details elsewhere (8). Briefly, HeLa cells adherent to glass slide were mounted onto an inverted microscope (Axiovert100, Zeiss), equipped with a 100× oil immersion objective (NA 1.4, Zeiss), and kept in PBS at 37°C. The apical membrane of the cells was observed. For imaging the 514 nm and 647 nm lines from an Ar/Kr laser (Spectra Physics) was coupled via an optical fiber into the excitation path of the inverted microscope. Images were taken consecutively for up to 1000 images per experiment. The time lag between images was varied between 11 and 69 ms. Precise timing and intensity setting for the excitation light was achieved by an acousto-optic tunable filter (AA Electrooptique). The illumination intensity was set to 2 kW/cm^2 and the illumination time per frame to 5 ms. The one dimensional positional accuracy achieved was $\sigma_x = \sigma_y = 25$ nm.

3.2.7 Data analysis

To analyze the data we applied particle image correlation spectroscopy (PICS), described in details in (9). This method is more robust when compared to tracking, as it is less affected by blinking and bleaching of the fluorophores. In short, the correlation between the positions at two different time lags is calculated. Corrections are applied to remove the contribution from randomly correlated molecules in close proximity to each other. This results in a cumulative probability function $P_{\text{cum}}(r^2, \Delta t)$ which yields the distribution of squared diffusive steps at a given time t. For each time lag, the P_{cum} is fitted to a two fractions model described by equation 3.1:

$$P_{\text{cum}}(r^2, \Delta t) = 1 - \left[\alpha \exp\left(-\frac{r^2}{4D_1\Delta t}\right) + (1-\alpha)\exp\left(-\frac{r^2}{4D_2\Delta t}\right)\right], \tag{3.1}$$

where $\text{MSD}_1 = 4D_1\Delta t$ is the characteristic mean square displacement of the fast diffusing fraction of size α and $\text{MSD}_2 = 4D_2\Delta t$ is the mean square displacement of the slow diffusing fraction of size $(1-\alpha)$. This double exponential model describe accurately the experimental curves.

3.3 Results

3.3.1 Mobility of Ifnar1 and Ifnar2 at stoichiometric concentration in presence and absence of stimulation

HeLa cells were transiently transfected with a plasmid containing both A1-Ifnar2-ΔIC and YFP-Ifnar1-ΔIC. Prior to measurements, A1-Ifnar2 was labeled with CoA-647 dye, as described in section 3.2. The two receptor components were depleted of the intracellular domain, thus the receptor was not signaling active. However, *in vitro* studies (6) show that this construct is still able to efficiently bind IFN and form a ternary complex. Single molecule microscopy was used to observe the diffusion of Ifnar1 and Ifnar2, both separately and simultaneously, at the apical membrane of HeLa cells. The apical membrane was chosen to minimize any effects that are potentially induced by interaction between the plasma membrane and the coverglass. Fluorescence images were taken up to 1000 consecutive frames, and the time delay between frames was varied between 11 and 69 ms. Single molecules were followed over time, and the positional accuracy achieved was $\sim$ 25 nm. PICS (9), as described in section 3.2, was subsequently applied to construct a cumulative probability function of the square displacements for a given time lag. The probability function for both Ifnar1 and Ifnar2 was best fitted by a two fraction model, which gives three parameters: fraction size α, which identifies a fast diffusing receptor population, characterized by a mean square displacement MSD_1, and a second slow moving population of size $1-\alpha$ with mean square displacement MSD_2 (see section 3.2).

In figure 3.1 the results for both Ifnar1 and Ifnar2 before and after stimulation are summarized. As shown in figure 3.1a, the fast moving population of Ifnar1 comprises $\alpha_{\mathrm{I1}} = 63 \pm 1\%$ of the total receptor population, while for Ifnar2 $\alpha_{\mathrm{I2}} = 70 \pm 3\%$. Upon stimulation with 5 nM IFNα2, no statistical significant change in fraction size was observed: $\alpha_{\mathrm{I1}}^{\mathrm{IFN}} = 54 \pm 8\%$ and $\alpha_{\mathrm{I2}}^{\mathrm{IFN}} = 74 \pm 1\%$, respectively. For both Ifnar1 and Ifnar2, the mean square displacement of the fast fraction does not increase linearly with time, thus was not representative of free diffusion (see figure 3.1). The data were best described assuming a confined diffusion model:

$$MSD(t) = \frac{L^2}{3}\left[1 - \exp\left(\frac{-12Dt}{L^2}\right)\right] + s_0 \tag{3.2}$$

where L is the confinement size, D the diffusion coefficient, t the time

lag, and s_0 is an offset which account for finite positional accuracy. In our experiments $s_0 = 4\sigma_x\sigma_y = 0.0049\ \mu\text{m}^2$.

Before stimulation the fast mobility of Ifnar1 is described by $L_{\text{I1}} = 753 \pm 27$ nm, and $D_{\text{I1}} = 0.508 \pm 0.042\ \mu\text{m}^2/\text{s}$ (figure 3.1b). After 15 minutes of stimulation with 5 nM IFNα2, the diffusive behavior changes: although the diffusion coefficient is unchanged within the experimental error $D_{\text{I1}}^{\text{IFN}} = 0.53 \pm 0.042\ \mu\text{m}^2/\text{s}$, the confinement size is reduced to $L_{\text{I1}}^{\text{IFN}} = 421 \pm 11$ nm (figure 3.1b), suggesting a tighter interaction between Ifnar1 and the membrane components upon stimulation with IFN. In the unstimulated case Ifnar1's slow fraction is immobile, or too slow to be detected above the limited positional accuracy, $D < 0.05\ \mu\text{m}^2/\text{s}$. Upon stimulation, however, diffusion of Ifnar1 is observed within domains of size $L_{\text{I1}}^{\text{slow}} = 231 \pm 10$ nm, with a diffusion coefficient $D_{\text{I1}}^{\text{slow}} = 0.067 \pm 0.01\ \mu\text{m}^2/\text{s}$ (see figure 2.1c).

Surprisingly, the results for Ifnar2 were strikingly different from what we observed for Ifnar1: the fast fraction before stimulation showed confined diffusion within big domains of size $L_{\text{I2}} = 637 \pm 19$nm, with diffusion coefficient $D_{\text{I2}} = 0.167 \pm 0.07\ \mu\text{m}^2/\text{s}$. Contrary to what was observed for Ifnar1, upon stimulation with IFNα2 the mobility did not change(figure 3.1b). The domain size was within the error the same as prior to stimulation, $L_{\text{I2}}^{\text{IFN}} = 668 \pm 11$nm while the diffusion coefficient was slightly higher compared to the unstimulated case, $D_{\text{I2}}^{\text{IFN}} = 0.29 \pm 0.08\ \mu\text{m}^2/\text{s}$. The slow fraction of Ifnar2 appears to be confined in small domains of size $L_{\text{I2}} = 190 \pm 28$nm, with a diffusion coefficient $D_{\text{I2}}^{\text{slow}} = 0.015 \pm 0.005\ \mu\text{m}^2/\text{s}$, and its mobility did not change upon stimulation, yielding $L_{\text{I2}}^{\text{IFN}} = 172 \pm 19$nm and $D_{\text{I2}}^{\text{IFN}} = 0.019 \pm 0.007\ \mu\text{m}^2/\text{s}$ (see figure 3.1c). Overall both Ifnar1 and Ifnar2, when expressed at stoichiometric concentration, are present in two distinct diffusing populations. One, fast diffusing fraction that is confined in big domain ranging in size between 600 and 750 nm. The second, slow moving fraction is confined in small domains of size $L \sim 200$ nm.

To ensure a ternary complex was formed upon stimulation with IFNα2, we performed cross-correlation experiments. In those measurements the fluorescence signals from Ifnar1 and Ifnar2 were imaged simultaneously onto separate areas of the CCD. Cross-correlation analysis (10) was applied to estimate the amount of complex formation. As shown in figure 3.1c, the cross-correlation experiments revealed the presence of a basal level of pre-formed ternary complex, corresponding to $\sim 20\%$ of the total receptor population. Upon stimulation with 5 nM IFNα2, an increase of

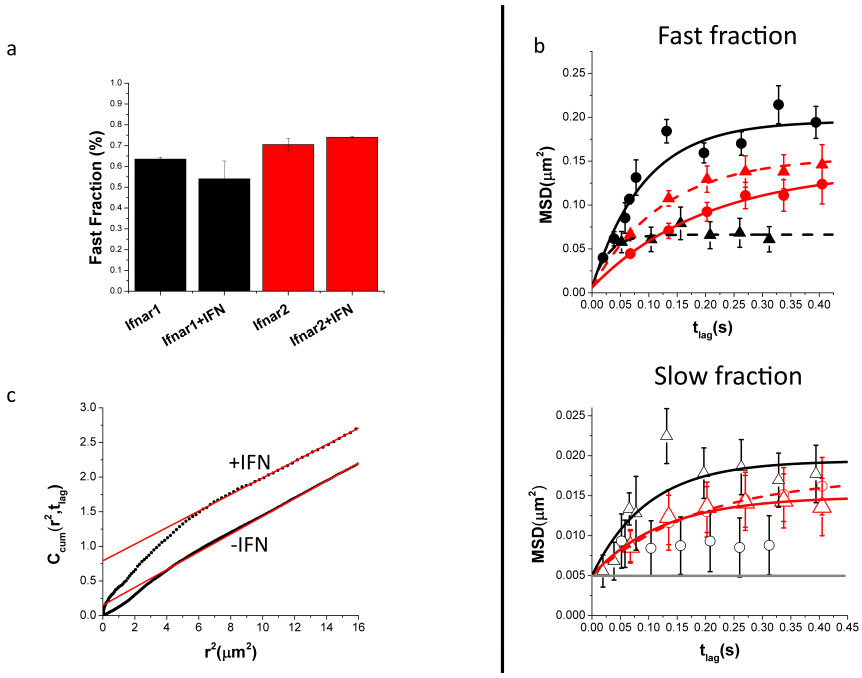

Figure 3.1: a) Fraction size for Ifnar1(black bars) and Ifnar2 (red bars), before and after stimulation with 5 nM IFNα2. Fraction size remains unchanged upon stimulation. **b)** Mean square displacement of Ifnar1 (black) and Ifnar2 (red). Top: fast fraction. Without stimulation: full circles. Upon stimulation with 5 nM IFNα2: full triangles. Both before (solid line) and after stimulation (dotted line) the data are best fitted with a confined diffusion model (see eqn.3.2). Bottom: slow fraction. Without stimulation: empty circles. Upon stimulation: empty triangles. **c** Cross-correlation curve shows a basal level ($\sim$ 20%) of pre-formed complexes. Upon stimulation, the level of cross-correlation increases up to $\sim$ 80%

.

the correlation between Ifnar1 and Ifnar2 up to 80% was observed, confirming the efficiency of the receptor components in living cell to form a ternary complex.

3.3.2 Effect of the actin cytoskeleton on receptor components mobility

To further explore the nature of the confinement observed, we performed a series of experiments where the actin cytoskeleton was disrupted by application of 0.6 μM latrunculin A (LatA). Cells were incubated for 10

minutes with LatA and subsequently imaged for 15 minutes in presence of LatA. Remarkably, no change in the fast fraction size of receptors was observed (see figure 3.2a), yielding $\alpha_{I1}^{LatA} = 56 \pm 4\%$, and $\alpha_{I2}^{LatA} = 67 \pm 3\%$ for Ifnar1 and Ifnar2 respectively. The diffusional behavior of both the fast and slow fraction of Ifnar1 was also unaffected by the treatment, as shown in figure 3.2c,d. On the contrary, the mobility of the fast diffusing population of Ifnar2 was greatly affected by actin disruption: the confinement observed in cell with intact actin cytoskeleton disappears, and Ifnar2 diffuses according to free Brownian motion with diffusion coefficient $D_{I2}^{LatA} = 0.807 \pm 0.07\ \mu\text{m}^2/\text{s}$, as shown in figure 3.2b. Ifnar2's slow diffusing population, instead, remains unchanged (see figure 3.2d).

Overall, these results indicate that the actin cytoskeleton is involved in Ifnar2 mobility, and that the domains observed were actin dependent. However, for Ifnar1 a different mechanism is required, or the interaction between actin and Ifnar1 is mediated by the intracellular domain which is depleted in our experiments. It is worth to highlight that the behavior of slow fraction for both Ifnar1 and Ifnar2 is unchanged upon actin disruption.

3.3.3 Ifnar2 mobility in absence of Ifnar1

HeLa cells were transiently transfected with a plasmid encoding only for A1-Ifnar2-ΔIC. This resulted in cells expressing high excess of Ifnar2 compared to the endogenous level of Ifnar1 present in HeLa cells (around 500 receptor subunits/cell). A1-Ifnar2 was labeled as described in section 3.2, and experiments were performed as described for the other construct. Measurement were performed in both unstimulated and stimulated cells. As in the case of Ifnar2 expressed at stoichiometric concentration as Ifnar2, the data were best fitted according to a two-population model. Figure 3.3 summarizes the results describing Ifnar2 mobility when expressed in high excess compared to Ifnar1.

Ifnar2 mobility was profoundly affected by the absence of Ifnar1 in our experiments. The fraction of Ifnar2 characterized by fast diffusion was lower than what we observed before: $\alpha_{\text{I2}}^{\text{single}} = 48 \pm 1\%$ compared to $\sim 63\%$ in presence of the other receptor subunit. Upon stimulation with 5 nM IFNα2 the fraction size remained unchanged, $\alpha_{\text{I2}}^{\text{singleIFN}} = 51 \pm 2\%$ as seen in figure 3.3a. The mean square displacement vs time graph highlight more differences between the mobility in presence and absence of Ifnar1. The fast population of the receptor subunit appears to be

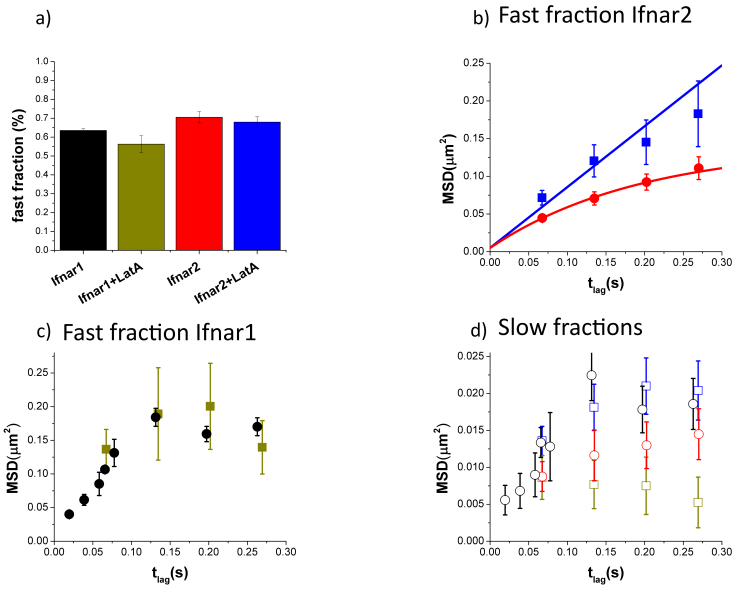

Figure 3.2: **a)**Fraction size before and after LatA treatment. There is not a statistical significant difference for both Ifnar1 and Ifnar2. **b)** Mean square displacement of Ifnar2's fast fraction before (red circles)and after LatA treatment (blue circles). Actin disruption results in the loss of confinement for Ifnar2.**c)** Mean square displacement of Ifnar1's fast fraction before (black circles), and after (olive circles). No significant change is observed in Ifnar1 mobility upon actin disruption. **d)** Ifnar1 and Ifnar2 slow fraction before and after actin disruption. No statistical significant change is observed for both Ifnar1 and Ifnar2.

confined into smaller domains, $L_{\mathrm{I2}}^{\mathrm{single}} = 459 \pm 20$ nm, and it is characterized by a diffusion coefficient $D_{\mathrm{I2}}^{\mathrm{single}} = 0.52 \pm 0.01\ \mu\mathrm{m}^2/\mathrm{s}$, faster than previously observed (see figure 3.3b). Upon stimulation with 5 nM IFNα2 the scenario changes drastically: the confinement size increases to $L_{\mathrm{I2}}^{\mathrm{singleIFN}} = 732 \pm 15$ nm, and the diffusion coefficient decreases to $D_{\mathrm{I2}}^{\mathrm{singleIFN}} = 0.24 \pm 0.007\ \mu\mathrm{m}^2/\mathrm{s}$. These results are directly comparable to what we measured for Ifnar2 co-expressed at stoichiometric concentration with Ifnar1. The slow diffusing fraction before stimulation is constantly below the positional accuracy ($s_0 = 0.0049\ \mu\mathrm{m}^2$), thus it is either immobile in the plane of the membrane, or its diffusion is too slow to be detected (figure 3.3c). Upon stimulation, we observed an increase in motility within domains of $L_{\mathrm{I2}}^{\mathrm{singleIFN}} = 116 \pm 11$nm, characterized by a diffusion coeffi-

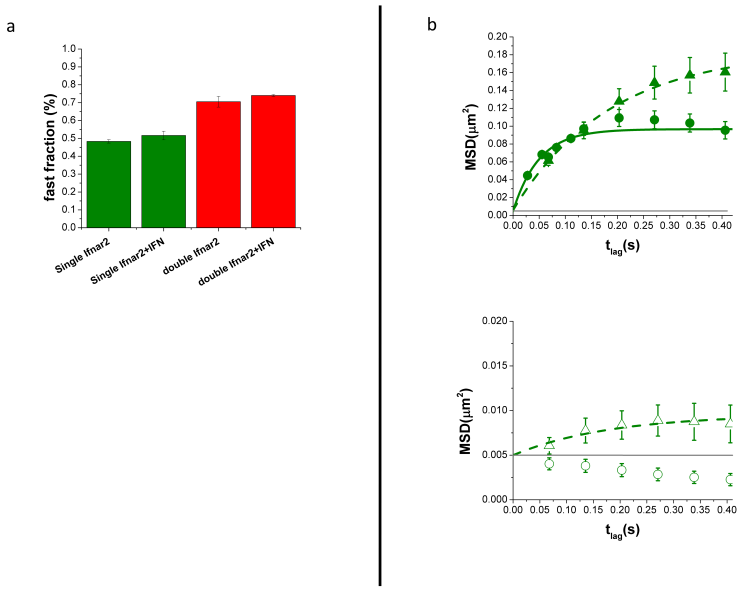

Figure 3.3: a) Fraction size for Ifnar2 expressed in high excess respect to Ifnar1 (green bars) and at stoichiometric concentration with Ifnar1(red bars), both before and after stimulation with 5 nM IFNα2. In absence of Ifnar1, a decrease in fraction size of $\sim 10\%$ is observed. In both cases, upon stimulation there is not a significant difference in fraction sizes. **b)** Mean square displacement of Ifnar2 in excess respect to Ifnar1. Top: fast fraction. Without stimulation: full circles. Upon stimulation with 5 nM IFNα2: full triangles. Both before (solid line) and after stimulation (dotted line) the data are best fitted with a confined diffusion model (see eqn.3.2). Bottom: slow fraction. Without stimulation: empty circles, Ifnar1 black, Ifnar2 red. Upon stimulation with 5 nM IFNα2: empty triangles.

cient $D_{\mathrm{I2}}^{\mathrm{singleIFN}} = 0.006 \pm 0.001 \mu m^2$, as depicted in figure 3.3. As for the fast moving population, these results resemble closely what was observed previously in the presence of Ifnar1.

3.3.4 Ifnar1 mobility in absence of Ifnar2

HeLa cells were transiently transfected with a plasmid encoding only for Ifnar1-eYFP-ΔIC. This resulted in cells expressing a high excess of Ifnar1 compared to the endogenous level of Ifnar2 present in HeLa cells (around 500 receptor subunits). Measurement were performed in both unstimulated and stimulated cells. As observed for the previous experimental conditions, the probability function was best fit by a two-population model.

In analogy to the results obtained for Ifnar2, the mobility of Ifnar1 when expressed in higher concentration with respect to Ifnar2 was greatly different from the case when the receptor components were expressed at a 1:1 ratio.

As illustrated in figure 3.4 a, the total amount of diffusing receptor increases, from $\alpha_{I1} \sim 54\%$ to $\alpha_{\mathrm{I1}}^{\mathrm{single}} = 71 \pm 1\%$. Upon stimulation with 5 nM IFNα2, the total amount of fast diffusing receptor was unchanged, yielding $\alpha_{\mathrm{I1}}^{\mathrm{singleIFN}} = 75 \pm 3\%$. Surprisingly, the mobility of Ifnar1 expressed in high excess resemble closely the one of Ifnar2 when expressed in high excess: as illustrated in figure 3.4 b. Before stimulation the subunits are confined in domains of size $L_{\mathrm{I1}}^{\mathrm{single}} = 389 \pm 5$nm, characterized by a diffusion coefficient $D_{\mathrm{I1}}^{\mathrm{single}} = 0.52 \ \ \mu\mathrm{m}^2/\mathrm{s}$. Due to the lack of data points at time lags shorter than 67 ms, the diffusion coefficient had to be taken as fixed parameter in the analysis. Upon stimulation with 5 nM IFNα2, the receptor subunits are no longer confined into small domains, but rather diffuses into much larger domains, with size $L_{\mathrm{I1}}^{\mathrm{singleIFN}} = 630 \pm 50$nm, with a diffusion coefficient $D_{\mathrm{I1}}^{\mathrm{singleIFN}} = 0.238 \pm 5 \ \ \mu\mathrm{m}^2/\mathrm{s}$. The slow fraction of Ifnar1 is, on the other hand, both before and after stimulation below the positional accuracy, indicating it is immobile or characterized by a diffusion coefficient too slow to be observed with our technique. It is worth to note, that although Ifnar1 behavior under these experimental conditions (absence of Ifnar2) strongly resembles the mobility of Ifnar2 under the same conditions, the changes observed are the opposite of what was observed when the receptor's components were present at stoichiometric concentration. Thus, taken together, these results suggest that in living cells differential stoichiometry between receptor components influence the mobility and the lateral organization of the subunits.

3.4 Discussion

The mechanism of type I Interferon receptor assembly has been extensively studied in the past years *in vitro*, yielding to a two-step ligand-induced receptor assembly model (6). Moreover, these studies highlighted the role of absolute and relative concentration of the ECD of the receptor subunits in ternary complex assembly on model membrane. However, how this process happens in living cells is still poorly understood. In this work we studied in detail the mobility of interferon receptor subunits, Ifnar1 and Ifnar2, in living HeLa cells by means of single molecule microscopy. We

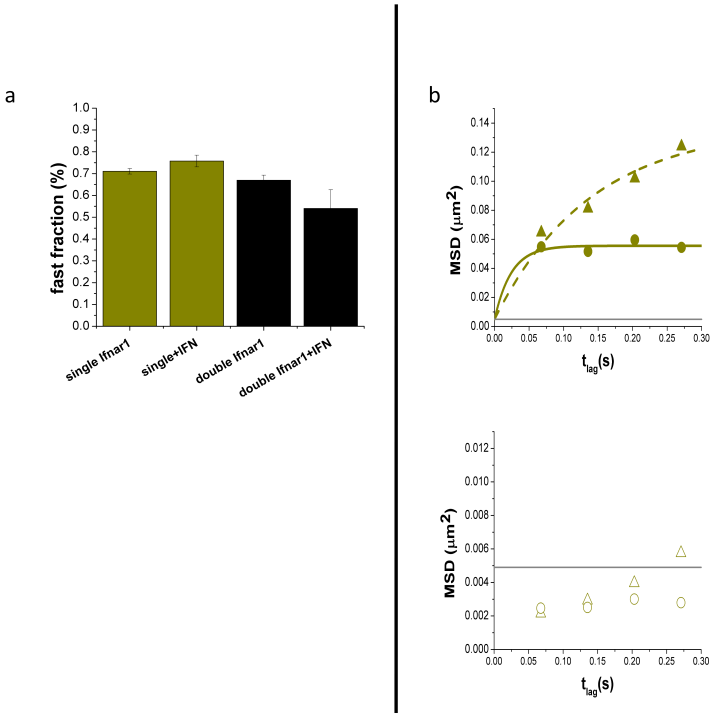

Figure 3.4: a) Fraction size for Ifnar1 expressed in high excess respect to Ifnar2 (olive bars) and at stoichiometric concentration with Ifnar2(black bars), both before and after stimulation with 5 nM IFNα2. In absence of Ifnar2, a decrease in fraction size of $\sim$ 10% is observed. In both cases, upon stimulation there is not a significant difference in fraction sizes. **b)** Mean square displacement of Ifnar1 in excess respect to Ifnar2. Top: fast fraction. Without stimulation: full circles. Upon stimulation with 5 nM IFNα2: full triangles. Both before (solid line) and after stimulation (dotted line) the data are best fitted with a confined diffusion model (see eqn.3.2). Bottom: slow fraction. Without stimulation: empty circles, Ifnar2 black, Ifnar1 red. Upon stimulation with 5 nM IFNα2: empty triangles.

gained insight into the parameter characterizing the mobility of each subunit, as well as information on their lateral organization in the membrane of living cells. The role of the actin cytoskeleton in the lateral organization of Ifnar and the effects of stimulation with IFNα2 were also analyzed.

Initially we studied the mobility of the two subunits expressed at stoichiometric concentration, 1:1 Ifnar1-ECD:Ifnar2-ECD, revealed the presence of two distinct populations of diffusing receptor components: a fast one, comprising the majority of the receptors (60-70%), whose motion is

confined in large domains of ∼700 nm, and a slower one, accounting for 30-40% of the receptor subunits, organized into smaller domains, ranging in size from ∼ 150 to 200 nm in size. The diffusion coefficients of the fast and slow fractions are in agreement with what observed previously for other membrane-anchored proteins (14). The segregation of receptor components in membrane domains has been previously suggested as a possible mechanism for increasing locally the concentration of Ifnar1 and Ifnar2, thus accounting for the high efficiency observed in subunits recruitment upon stimulation (4, 7). However, the association of the receptor subunits with lipid microdomains has been observed only through biochemical studies (11–13), particularly for type II interferon receptor subunits. Co-precipitation experiments showed that Ifnar1 is found in caveolae-like microdomains, which plays a fundamental role in nuclear translocation and in the early stages of interferon signaling. However, up to date, direct observation of confinement in these domains has not been reported(13). Given the small size of caveolae, ranging from 60 to 150 nm, as illustrated in (14), it is suggestive to identify the slow diffusing fraction with the caveolae-associated receptors. The work of Marchetti (11) showed how upon IFNα2 binding the amount of Ifnar1 in detergent resistant membrane did not increase. This is consistent with the observation in our results that the fraction size remains unchanged upon stimulation. However, our experiments were able to show an effect on the mobility of Ifnar1-ECD upon stimulation with IFNα2 which was not possible to observe previously. Although the absence of the ICD makes unlikely that the effect observed is caused by phosphorylation of Ifnar1, the increase in diffusion coefficient and confinement size could be due to the IFNα-induced recruitment of STAT2 to Ifnar1 (1). Interestingly, in Ifnar2 mobility we did not observe any change upon IFNα2 stimulation.

The confinement size of the fast fraction, instead, is too large to be originating from lipid-domain association. Since previous work suggested an association with the actin cytoskeleton for the receptor subunits of type II interferon receptor, we investigated whether the actin cytoskeleton was responsible for the large domains we observed. Indeed, depletion of F-Actin by administration of LatA to cells, partially confirmed our hypothesis: upon actin disruption, Ifnar2 but not Ifnar1, began to diffuse according to Brownian motion, with an increased diffusion coefficient $D_{I2}^{LatA} = 0.8\ \mu\text{m}^2$. Although the mobility of the fast fraction of Ifnar2 is deeply affected by LatA treatment, neither the size of the population

nor the mobility of the slow fraction are changed by toxin application, supporting the identification of the slow fraction with caveolin-associated receptor. Thus, these results support the hypothesis that interaction with different membrane components is responsible for the biphasic behavior observed. In the work of Cruz et al. (16), it was reported how modification and truncation of the intracellular domain of IFNγ-R1 abrogated the ability of colocalization with the actin filaments. Since the receptor subunits are lacking the ICD, different anchoring point to the actin cytoskeleton could account for the differences observed between Ifnar2 and Ifnar1 upon LatA treatment. Likewse, interaction between Ifnar1 and downstream signaling components could also play a role in maintaining the lateral segregation even upon actin disruption.

It is worth to note how IFNα2 stimulation also effects differently the receptor's subunits mobility. While for Ifnar2 no significant change was detected, Ifnar1 mobility was largely affected by stimulation. The confinement size was reduced, whilst the diffusion coefficient was unchanged within the experimental error. These observation suggests once more that the confinement observed for Ifnar1 is due to interaction with downstream signaling components, such as STAT1, and not to association with the actin cytoskeleton.

Cross-correlation experiments confirmed that there is no pre-association of the ECD of the two subunits, although a minimal level ($\sim$20%) of pre-coupled complexes was detected.

Finally, we assessed the role of the relative concentration for the lateral organization and mobility of the receptor subunits. Works from the group of Piehler (5–7), showed the influence of the relative and absolute concentration of the Ifnar1-ECD and Ifnar2-ECD on ternary complex assembly and stability in solid supported membrane. It was suggested that the differential responsiveness to IFNs is modulated by the concentration of Ifnar1. If its concentration is too low, the recruitment into the ternary complex is highly inefficient due to the low affinity for IFNα. Here, we compared the mobility of Ifnar1-ECD and Ifnar2-ECD expressed in higher excess respect one another with the 1Ifnar1-ECD:1 Ifnar2-ECD stoichiometry experiments. In both cases, the high excess of one subunit induces a change in its mobility, and the results for single Ifnar1 and single Ifnar2 are strikingly similar. Before stimulation the receptor subunits are confined in domains smaller ($L \sim 400$nm) than in the stoichiometric case. The decrease in domain size is associated with an increase in diffusion

coefficient (D=0.52 μm^2/s) for Ifnar2. Upon stimulation, we observed an increase in confinement size ($L \sim 630 - 700$nm), and a corresponding decrease in diffusion coefficient for both subunits ($D \sim 0.25$ μm^2/s). While for Ifnar1 the slow fraction is (both before and after stimulation) below the positional accuracy, for Ifnar2 we observe an increase in mobility upon stimulation. Taken together with the results from cross-correlation experiments, these findings suggest that although there is no pre-coupling of the receptor subunits, a transient interaction in the plane of the membrane might play a role in maintaining the lateral organization of receptor components.

In conclusion, we show that interactions between receptor subunits, their relative stoichiometry, and different membrane components are fundamental for maintaining the lateral organization of components in the membrane. It is highly likely that the lateral organization is of utmost importance for a faithful and efficient complex assembly in interferon signaling.

Bibliography

[1] Borden, E. C., Sen, G. C., Uze, G., Silverman, R. H., Ranshoff, R. M., Foster, G. R., Stark, G. R. (2007) Interferons at age 50: Past, Current and Future Impact on Biomedicine. *Nat. Rev. Drug. Disc.* **6**, 975-990.

[2] Chill, J. H., Quadt, S. R., levy, R., Schreibert, G., Anglister, J. (2003) The human type I interferon receptor: NMR structure reveals the molecular basis of ligand binding. *Structure* **11-7**, 791-802.

[3] Kotenko, S.V., Langer, J. A. (2004) Full house: 12 receptors for 27 cytokines. *Int. Immuno-pharmacol.* **4**, 593-608.

[4] Uze, G., Schreiber, G., Piehler, J., Pellegrini, S. (2007) The Receptor of the Type I Interferon Family. *Curr. Top. Microbiol. Immunol.* **316**, 71-95.

[5] Lamken, P., Lata, S., Gavutis, M., Piehler, J. (2004) Ligand-Induced Assembling of the Type I Interferon Receptor on Supported Lipid Bilayers. *J. Mol. Biol.* **366**, 525-539.

[6] Gavutis, M., Jaks, E., Lamken, P., Piehler, J. (2006) Determination of the Two-Dimensional Interaction Constants of a Cytokine Receptor Complex. *Biophys. J.* **90**, 3345-3355.

[7] Gavutis, M., Lata, S., Lamken, P., Muller, P., Piehler, J (2005) Lateral ligand-receptor interaction on membranes probed by simultaneous fluorescence-interference detection. *Biophys. J. textbf*88, 4289-4302.

[8] Harms, G. S., Cognet, L., Lommerse, P. H., Blab, G. A., Schmidt, T. (2001). Autofluorescent proteins in single-molecule research: Applications to live cell imaging microscopy. *Proc. Nat. Acad. Sci.* **80**, 2396 - 2408.

[9] Semrau, S., Schmidt, T. (2007) Particle image correlation spectroscopy (PICS). Retrieving nanometer-scale correlations from high-density single-molecule position data. *Biophys J.* **92**, 613-621.

[10] Semrau, S., Holtzer, L., Gonzalez-Gaitan, M., Schmidt, T. (2011) Quantification of biological interactions with Particle Image Cross Correlation Spectroscopy (PICCS). *Biophys. J.* **100**, 1810-8.

[11] Marchetti, M., Monier, M-N., Fradagrada, A., Mitchell, K., Baychelier, F., Eid., P., Johannes, L., Lamaze, C. (2006) Stat-mediated singnaling induced by type I and type II interferons (IFNs) is differentially controlled though lipid microdomains association and clathrin-dependent endocytosis of IFNs receptors. *Mol.Biol.Cell.* **17**, 2896-2909.

[12] Subramaniam, P. S., Johnson, H. M. (202) Lipid microdomains are required sites for the selective endocytosis and nuclear translocation of IFN-γ, its receptor chain IFN-γ receptor-1, and the phosphorylation and nuclear translocation of STA1α. *J. Imm.* **169**, 1959-1969.

[13] Takaoka, A., Mitani, Y., Suemori, H., Sato, M., Yokochi, T., Noguchi, S., Tanaka, N., Taniguchi, T. (2000) Cross talk between interferon-γ and -α/β signaling components in caveolar membrane domains. *Science* **288**, 2357-2360.

[14] Lommerse, P. H. M., Spaink, H.P., Schmidt, T. (2004) In vivo plasma membrane organization: results of biophysical approaches. *Biochem. et Biophys. Acta*, **1664**, 119-131.

[15] Pfeffer, L. M., Stebbing, N., Donner, D. B. (1987) Cytoskeletal association of human α-interferon-receptor complexes in interferon-sensitive and -resistant lymphoblastoid cells. *Prot. Natl. Acad. Sci. USA* **84**, 3249-3253.

[16] Cruz, M., Hernandez, J. M., Calderon, J. (1998) Surface redistribution of interferon γ-receptor and its colocalization with the actin cytoskeleton. *Arch. Med. Res.* **30**, 97-105.